Lifetime statistics of quantum chaos studied by a multiscale analysis

A. Di Falco, T. F. Krauss, and A. Fratalocchi
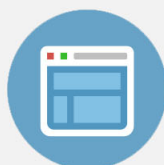
Lifetime statistics of quantum chaos studied by a multiscale analysis

A. Di Falco,[1] T. F. Krauss,[1] and A. Fratalocchi[2,a)]

[1]School of Physics and Astronomy, University of St. Andrews, North Haugh, St. Andrews, KY16 9SS, United Kingdom
[2]PRIMALIGHT, Faculty of Electrical Engineering, Applied Mathematics and Computational Science, King Abdullah University of Science and Technology (KAUST), Thuwal 23955-6900, Saudi Arabia

In a series of pump and probe experiments, we study the lifetime statistics of a quantum chaotic resonator when the number of open channels is greater than one. Our design embeds a stadium billiard into a two dimensional photonic crystal realized on a silicon-on-insulator substrate. We calculate resonances through a multiscale procedure that combines energy landscape analysis and wavelet transforms. Experimental data is found to follow the universal predictions arising from random matrix theory with an excellent level of agreement. © 2012 American Institute of Physics. [http://dx.doi.org/10.1063/1.4711018]

In a seminal paper of 1917, Albert Einstein provided a remarkable insight about the failure of energy quantization schemes when applied to nonintegrable systems and raised the question "*Does chaos lurk in the smooth, wavelike, quantum world*?"[1,2] This problem was practically ignored until 1970, when theoretical physicists led by Gutzwiller investigated the implications of classical chaos for semiclassical quantum systems and founded the research field known as quantum chaos. Besides quantum mechanics, the problem posed by Einstein is of great importance due to the large number of systems that can be treated semiclassically.[3] Among them, electromagnetic waves have stirred particular interest. In electrodynamics, quantum chaos originates from the isomorphisms between Schrödinger and Maxwell's equations in two spatial dimensions and is manifested in resonators whose forms mimic classically chaotic billiards. In these geometries, semiclassical methods and random matrix theory (RMT) provide theoretical predictions that have found to well agree with several experiments, leading not only to fundamental discoveries but also to applications in the field of laser devices.[3–9] One of the most fundamental aspects of quantum chaos lies in the universality of its eigenmodes, first conjectured by Bohigas, Giannoni, and Schmit in 1984 for closed systems[10] and then theoretically extended to open media (originally discussed in the context of nuclear physics) through random matrix theory.[11] According to RMT, the spectral resonances of a quantum chaotic system show universal probability distributions, which depend only on the symmetries of the original equation and the number of open channels $\mathcal{N}$ considered.[12,13] However, while there exists a large experimental literature on the study of the position of each resonance (i.e., the real part of the eigenvalue of an eigenmode, see Ref. 3 and references therein), experimental work on the lifetime statistics (i.e., the imaginary part, or equivalently, the resonance width) is still at the beginning. The measurement of the lifetimes, in fact, is an extremely challenging task due to resonances overlapping in the eigenmodes spectrum. In this field of research, the present literature consists only of two experiments at microwave

frequencies.[14,15] A comparison between RMT and experimentally measured lifetime probability distributions has been attempted for a system with a single open channel ($\mathcal{N} = 1$), showing a behavior whose physical origin is still not understood.[14] Besides that, the case $\mathcal{N} > 1$ (where the form of the statistics is strongly different from the case $\mathcal{N} = 1$) has never been addressed yet, as well as an experimental analysis at optical wavelengths, which are the ideal playground to develop applications as well as to study the interplay of quantum chaos with fundamental physical effects such as different forms of nonlinear material responses (see, e.g., Refs. 6 and 9).

In this letter, we study the lifetime statistic of a chaotic optical microresonator in the case of $\mathcal{N} > 1$. In a series of pump and probe experiments, we injected a broadband source signal into a stadium microresonator and collected the output by a fiber spectrograph. Resonance lifetimes have then been extracted from the power spectrum by a multiscale procedure which combines wavelet transforms and energy landscape analysis.[16,17] We performed an experimental campaign on five different samples, and analyzed more than 700 resonances. Experimentally measured statistics were found to perfectly match the universal predictions of RMT.

Experiments on wave chaos have been traditionally performed in the microwave regime due to possibility of using large geometries ($\approx$ mm) and low loss metals acting as mirrors. At optical wavelengths, conversely, metals are lossy and low absorption dielectrics should be employed. However, a naive implementation of a chaotic billiard with dielectrics results into large Fresnel losses, and RMT statistics would no longer be universal.[18] In order to overcome this problem ad design, an optical cavity that mimics a microwave billiard, we resorted to photonic crystals (PhCs) technology.[19,20] In particular, we embedded a fully chaotic stadium geometry in a two dimensional photonic crystal made by a triangular lattice of cylindrical air holes in silicon (Fig. 1). The sample was fabricated on a silicon on insulator substrate, with a SiO$_2$ buffer layer of 2 μm and a silicon capping layer of 220 nm. The PhC pattern was written with a standard lithographic procedure, involving exposure with an e-beam system, development of the photoresist, and

a)URL: www.primalight.org

transferring of the pattern on to the substrate with reactive ion etching step (see, e.g., Ref. 21). The confinement in the transverse direction is guaranteed by total internal reflection, whereas the PhC cavity ensures light confinement in the plane. The sample was designed to work with the electric field parallel to the surface (TE modes). Inside a photonic crystal, wavelengths λ that fall in the PhC gap $\Delta\lambda$ cannot propagate due to a zero density of electromagnetic states.[19] In such a frequency range, light energy entering into the billiard gets totally reflected by the PhC walls and escapes in the input and output waveguides.

In order to collect a sufficiently large statistics, we designed different samples with the same billiard area (of 700 μm^2) and diverse filling factor $f = \frac{r}{a}$, r being the radius of the single air hole and a the lattice spacing (Fig. 1). By varying the filling factor in the range $f \in [0.25, 0.3]$, we guaranteed a photonic bandgap for electromagnetic TE modes of $\Delta\lambda > 400$ nm, which is sufficiently larger than the bandwidth of the laser source employed for the experiments. The experimental setup consisted of a polarized C + L band amplified spontaneous emission source (central wavelength 1575 nm, bandwidth 110 nm), which injected light into a single mode fiber that was coupled to the sample by a 60× aspheric lens, with antireflection coating. Light emerging from the output channel was then collimated by a 40× aspheric lens into a second single mode fiber, split between a photodetector (to monitor the coupling optimization) and an ANDO optical spectrum analyzer. All spectra were acquired with a resolution of 10 pm. Figure 2 shows a typical power density spectrum $\mathcal{P}(\lambda)$ obtained from a single measurement. We observe strong clustering effects, with several resonances overlapping in the spectrum (see Fig. 2(b)). We emphasize that, due to such overlapping and the impossibility of measuring the time evolution of the photon's carrier at optical frequencies, no standard method of resonances extraction (such as, e.g., the harmonic inversion employed in Ref. 14) could be employed. For this reason, we developed an original approach that exploits ideas from multiresolution analysis[16] and complex landscapes topology.[17] More specifically, we begin by applying a continuous wavelet transform $(\mathcal{WP})(\zeta, s)$ to the power density spectrum $\mathcal{P}$,

$$(\mathcal{WP})(\zeta, \chi) = \int_{-\infty}^{\infty} \mathcal{P}(\lambda) \frac{1}{\sqrt{\chi}} \psi\left(\frac{\lambda - \zeta}{\chi}\right) d\lambda, \qquad (1)$$

χ, ζ being scaling and translation parameters, respectively, and ψ the so-called mother wavelet, which is a compact function in $L^2(\mathbf{R})$ possessing a zero mean value and satisfying $\int_{-\infty}^{\infty} \frac{|\tilde{\psi}(f)|^2}{|f|} df < \infty$ ($\tilde{\psi}$ denotes the Fourier transform of ψ). To extract Lorentzian-like linewidths out of the spectrum, we choose the following symmetric wavelet $\psi = (2 - 4t^2)e^{-t^2}$, which is defined from the second derivative of a Gaussian function. The integral transform (1), when applied to the power density spectrum resulting from a measurement, provides a geometric visualization of the inner structure of the spectral resonances—given by the regions of high density in Fig. 3—which change according to the scale χ considered. As χ increases, resonances found at smaller scales evolve into tree-like structures and eventually join together (Fig. 3(b)). The topology of the surface $(\mathcal{WP})$ encodes the structure of all the resonances of the system. Isolated resonances, in particular, are observed due to the missing of any tree structure in $(\mathcal{WP})$, while a link between high-density regions is the signature of the presence of a cluster. We describe clusters and isolated resonances by an uphill landscape analysis[17] applied to the wavelet transform. Figure 4(a) illustrates this analysis when applied to the portion of the spectrum of Fig. 2(b). In particular, we employ a series of runners (Fig. 4(a), solid lines), which evolve along χ following the curve of minimum steepness on the surface $(\mathcal{WP})$, and nodes (Fig. 4(a), circle dots) denoting the intersection among different runners. We geometrically describe tree-like structures among paths of different runners by building an adjacency matrix $\mathcal{A}$, with $\mathcal{A}_{ij} = 1$ if the path of runners i and j overlaps, and $\mathcal{A}_{ij} = 0$ otherwise. The matrix $\mathcal{A}$ carries the information on both the structure and the composition of all the clusters of resonances in the spectrum. In conjunction with the wavelet transform $(\mathcal{WP})$, it provides the required knowledge to extract position and spectral linewidth of the billiard eigenmodes. Isolated resonances, characterized by $\mathcal{A}_{ij} = 0$ for $j \neq i$, are described by following the path of the corresponding runner up to the first maximum in the surface $(\mathcal{WP})$, which yields the highest
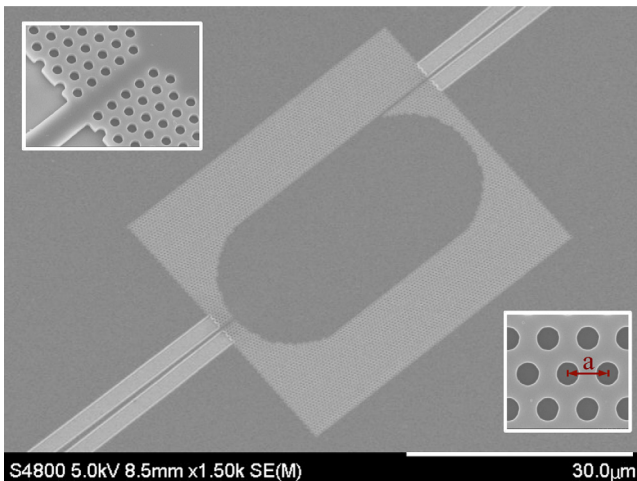

FIG. 1. SEM image of the open stadium billiard realized within a two dimensional photonic crystal. Insets represent magnified details of the sample: (top) input waveguide and (bottom) triangular lattice.

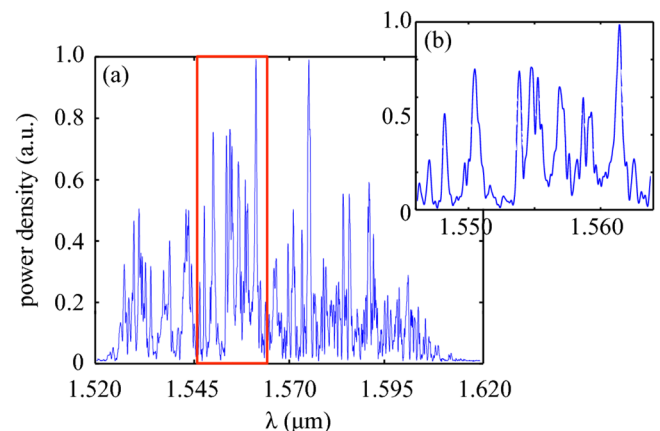FIG. 2. (a) Experimental power density spectrum $\mathcal{P}(\lambda)$ retrieved for a sample with $f = 2.88$; (b) enlarged portion (a) for $\lambda \in [1.546\ \mu m, 1.564\ \mu m]$.

overlap according to the L^2 distance defined by Eq. (1). At the maximum point in the plane (χ, ζ), the full width half maximum (FWHM) linewidth $\delta\lambda$ is $\sqrt{2\log 2}$ times the waist of the Gaussian part of the wavelet, and reads $\delta\lambda = \chi\sqrt{\log 2/2}$, while the resonance position λ_0 is given by $\lambda_0 = \zeta$. In the presence of resonance clusters, which show nonzero connections in the adjacency matrix (i.e., $A_{ij} \neq 0$ for $j \neq i$), we found optimal $(\lambda_0, \delta\lambda)$ by a nonlinear simplex optimization search in the subspace spanned by the runners path in the plane (χ, ζ) of the surface $(\mathcal{WP})$. Stemming from the theoretical parameters $(\lambda_0, \delta\lambda)$ obtained through the combined analysis on $(\mathcal{WP})$ and A, we finally apply a global nonlinear least-square optimization across the entire spectrum for further increasing the fidelity of our estimated results. The outcome of this procedure is quite satisfactory. Figure 4(b) compares a portion of the theoretical spectrum reconstructed by the method described above and the experimental measure. As seen, the experimental data is barely visible due to an excellent agreement with the fitted curve obtained through the multiscale analysis. We highlight that all experimental spectra (not shown here) were reconstructed with the same degree of precision. Figure 5 reports the distribution of the resonances in the plane $(\lambda_0, \delta\lambda)$ for the five samples considered in our experiments. The figure shows a clear separation of the resonance dynamics into two different regions. A few, isolated short living resonances and many long living modes with positions are completely random in $(\lambda_0, \delta\lambda)$ and do not overlap in the plane (Fig. 5(b)), thus witnessing statistical independence of the acquired data. In order to compare our results to the corresponding quantum-mechanical predictions, we begin by expressing the scattering matrix $S(\mathcal{E})$,[14,22] which relates the vector of incoming $\mathbf{B}$ and outgoing $\mathbf{A}$ electromagnetic field amplitudes by $\mathbf{B} = S\,\mathbf{A}$ with $S(\mathcal{E}) = 1 - 2\pi i \mathcal{W}(\mathcal{E})^{\dagger}\,\mathcal{D}(\mathcal{E})^{-1}\mathcal{W}(\mathcal{E})$, $\mathcal{E}$ playing the role of a quantum-mechanical energy, $\mathcal{W}$ the operator modeling the coupling with the environment (i.e., the channel space), and $\mathcal{D} = \mathcal{E} - \mathcal{H}_0 + i\pi\mathcal{W}\mathcal{W}^{\dagger}$, $\mathcal{H}_0 = \nabla^2 + k^2$ being the Hamiltonian corresponding to the close billiard. Resonances of the system originate from the poles of the scattering matrix S and, therefore, from the eigenvalues $\mathcal{E} = \nu - i\gamma$ of $\mathcal{H}_0 - i\pi\mathcal{W}\mathcal{W}^{\dagger}$. The eigenvalues imaginary part γ, which corresponds to the distribution of the resonances width of the open chaotic system, can be related to the electromagnetic measured data $(\lambda_0, \delta\lambda)$ from the relation $k^2 = \frac{\omega^2}{c^2} = \mathcal{E}$, and reads $\gamma = \delta\lambda/\lambda_0^3$ (omitting inessential proportionality constants). In our PhC geometry, open channels originate inside all the leaky ele-
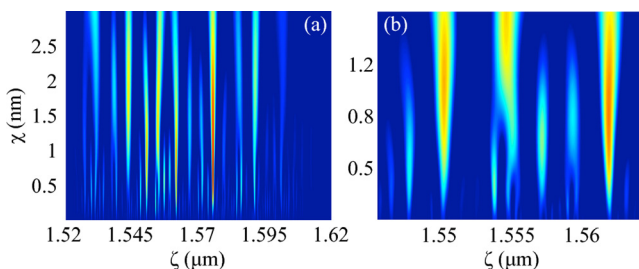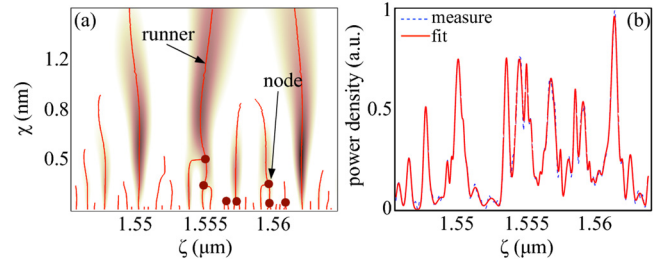

FIG. 4. (a) Uphill pathways analysis (runners as solid lines and nodes as circle markers) of the wavelet transform of Fig. 3(b), reported for reference as pseudocolor plot; (b) theoretical reconstructed spectrum versus experimental measure.

ments of the structure (i.e., waveguides, surfaces, and PhC itself due to it finite extension). All these elements are sources of weakly—and evanescently small—energy leakage outside the billiard. It is worthwhile stressing that the physical mechanism underlying all losses in our structure is the same (i.e., evanescent coupling between the cavity mode and the radiation or guided modes), while absorption is totally negligible due to the transparency of Si in the infrared region. All open channels can be, therefore, treated on the same physical basis, where each of them is weakly coupled to the external environment. In this condition, the width probability function $p(\gamma)$ reads[13,23] $p(\gamma) = \int_{-\infty}^{+\infty} \frac{dk}{2\pi} \frac{e^{-ik\gamma}}{\sqrt{\det|1 - ik\mathcal{G}|}}$, with $\mathcal{G}$ being a $\mathcal{N} \times \mathcal{N}$ matrix expressing the correlations among the channels. In general, we do not expect any correlation among losses due to the fact that they occur in both random directions and uncorrelated space regions. We, therefore, can further simplify the previous equation in the limit, where $\mathcal{G}$ is diagonal, with $\mathcal{G}_{ij} = \delta_{ij}/g$. Straightforward integration yields

$$p(\gamma) = \frac{g^{\mathcal{M}}}{\Gamma(\mathcal{M})}\gamma^{\mathcal{M}-1}e^{-g\gamma}, \qquad (2)$$

with $\mathcal{N}/2 = \mathcal{M}$ and $g = (2\mathcal{M}\langle\gamma\rangle)^{-1}$. The distribution equation (2) is universal and uniquely determined by $\mathcal{M}$. This coincides with the same distribution employed in Ref. 14 to keep into account losses, although derived by means of another approach. Figure 6 compares the experimentally measured distribution of γ with the theoretical prediction of RMT with $\mathcal{M} = 5$, which produces the best fit (in a least-square sense) of the experimental data. As seen, an

FIG. 3. (a) and (b) Continuous wavelet transform of the power density spectrum $\mathcal{P}(\lambda)$ of Figs. 2(a) and 2(b), respectively.
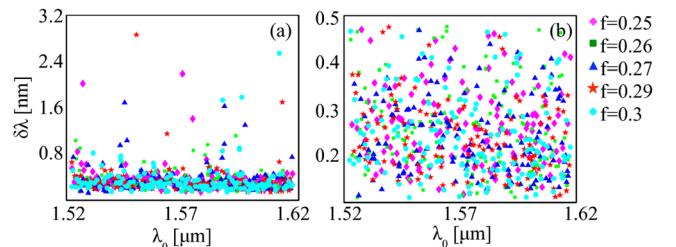

FIG. 5. (a) and (b) Position λ_0 and FWHM linewidth $\delta\lambda$ of chaotic resonances extracted by the multiscale analysis. (b) A magnified version of (a) in the region where the resonances exhibit a random behavior. In (a) and (b), different markers (colors) refer to different filling factors f (see the legend on the right).
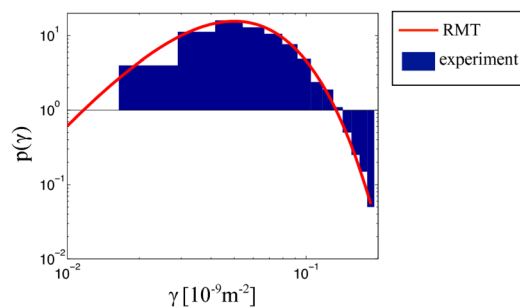
FIG. 6. Log-Log distribution of resonance imaginary part $p(\gamma)$ (histogram) and theoretical prediction arising from RMT (solid line).

excellent level of agreement is found (of almost three orders of magnitude) between theory and experiments. The sources of losses behave as $\mathcal{N} = 10$ equivalent weakly channels.

In conclusion, motivated by a question posed by Einstein in the last century, we investigated the universal behavior of quantum systems in the presence of deterministic chaos. We designed and experimentally characterized photonic crystal resonators that are fully equivalent to open quantum billiards. Our experimental results, analyzed within a theoretical framework that combines ideas from multiresolution analysis, unambiguously demonstrate the existence of universal statistics in the lifetime of quantum chaos. Universality is a concept of utmost importance in every branch of physics, and its implications at the quantum scale are fundamental not only to add a piece to the puzzle initiated by Einstein's intuition, but also to give rise to quantum devices that exploit universal phenomena and operate regardless of their microscopic details.

[1] *The Collected Papers of Albert Einstein, The Berlin Years: Writings* Vol. 6, edited by A. J. Kox, M. J. Klein, and R. Schulmann (Princeton University Press, New Jersey, 1996), pp. 1914–1917.
[2] M. Gutzwiller, Sci. Am. **266**, 78 (1992).
[3] H. J. Stöckmann, *Quantum Chaos: An Introduction* (Cambridge University Press, Cambridge, 2007).
[4] T. Gensty, K. Becker, I. Fischer, W. Elsäßer, C. Degen, P. Debernardi, and G. P. Bava, Phys. Rev. Lett. **94**, 233901 (2005).
[5] J. U. Nöckel and A. D. Stone, Nature (London) **385**, 45 (1997).
[6] C. Gmachl, F. Capasso, E. E. Narimanov, J. U. Nöckel, A. D. Stone, J. Faist, D. L. Sivco, and A. Y. Cho, Science **280**, 1556 (1998).
[7] C. Michel, V. Doya, O. Legrand, and F. Mortessagne, Phys. Rev. Lett. **99**, 224101 (2007).
[8] T.-D. Lee, C.-Y. Chen, Y. Lin, M.-C. Chou, T.-H. Wu, and R.-K. Lee, Phys. Rev. Lett. **101**, 084101 (2008).
[9] C. C. Chen, Y. T. Yu, R. C. C. Chen, Y. J. Huang, K. W. Su, Y. F. Chen, and K. F. Huang, Phys. Rev. Lett. **102**, 044101 (2009).
[10] O. Bohigas, M. J. Giannoni, and C. Schmit, Phys. Rev. Lett. **52**, 1 (1984).
[11] J. Verbaarschot, H. Weidenmüller, and M. Zirnbauer, Phys. Rep. **129**, 367 (1985).
[12] T. Guhr, A. Müller-Groeling, and H. A. Weidenmüller, Phys. Rep. **299**, 189 (1998).
[13] H.-J. Sommers, Y. V. Fyodorov, and M. Titov, J. Phys. A **32**, L77 (1999).
[14] U. Kuhl, R. Höhmann, J. Main, and H.-J. Stöckmann, Phys. Rev. Lett. **100**, 254101 (2008).
[15] H. Alt, H. D. Gräf, H. L. Harney, R. Hofferbert, H. Lengeler, A. Richter, P. Schardt, and H. A. Weidenmüller, Phys. Rev. Lett. **74**, 62 (1995).
[16] S. Jaffard, Y. Meyer, and R. D. Ryan, *Wavelets: Tools for Science & Technology* (SIAM, Philadelphia, 2001).
[17] D. J. Wales, *Energy Landscapes* (Cambridge University Press, Cambridge, 2003).
[18] J. P. Keating, M. Novaes, and H. Schomerus, Phys. Rev. A **77**, 013834 (2008).
[19] K. Sakoda, *Optical Properties of Photonic Crystals* (Springer-Verlag, Berlin, 2001).
[20] D. Labilloy, H. Benisty, C. Weisbuch, T. F. Krauss, R. M. De La Rue, V. Bardinal, R. Houdré, U. Oesterle, D. Cassagne, and C. Jouanin, Phys. Rev. Lett. **79**, 4147 (1997).
[21] A. D. Falco, L. O'Faolain, and T. F. Krauss, Appl. Phys. Lett. **92**, 083501 (2008).
[22] H. L. Harney, F. M. Dittes, and A. Müller, Ann. Phys. **220**, 159 (1992).
[23] Y. Alhassid and C. H. Lewenkopf, Phys. Rev. Lett. **75**, 3922 (1995).